Laser Induced Phased Arrays for remote ultrasonic imaging of additive manufactured components

Theodosia Stratoudaki, Yashar Javadi
Department of Electronic and Electrical Engineering, University of Strathclyde
Glasgow, G1 1XW, UK
Telephone: +44 (0)141548 4397
E-mail: t.stratoudaki@physics.org

William Kerr
Advanced Forming Research Centre (AFRC), University of Strathclyde
Renfrew, PA4 9LJ, UK

Paul D. Wilcox
Department of Mechanical Engineering, University of Bristol
Bristol, BS8 1TR, UK

Don Pieris, Matt Clark
Department of Electrical and Electronic Engineering, University of Nottingham
Nottingham, NG7 2RD, UK

Abstract

Laser Induced Phased Arrays (LIPAs) use laser ultrasonics to generate and detect ultrasound, synthesising an ultrasonic phased array in post processing. Full Matrix Capture (FMC) is done by scanning the laser generation and detection beams at every possible combination with respect to position. The acquired data are used to synthesise a focus at every point in the section imaged, using the Total Focusing Method (TFM). The result is greatly improved imaging quality compared to conventional laser ultrasonic imaging. As the technique is remote and couplant free it lends itself well to extreme environments, such as the Additive Manufacturing (AM) process.
We will present remote ultrasonic TFM images of additive manufactured components made of aluminium, using Selective Laser Melting (SLM). LIPAs were synthesised under the base plate of the built, to demonstrate the capability for in situ process monitoring. The aluminium built incorporated six side through holes of 0.5-1mm diameter size, in its design, in order to simulate process occurring defects. These were located as deep as 25mm below the surface of the component and were successfully imaged using LIPAs. TFM images from transducer based phased arrays will also be presented to complement the analysis.

1. Introduction

Additive Manufacturing (AM) is steadily developing into a mainstream manufacturing technology due to its capability to manufacture complex geometries, compared to casting and cost savings compared to subtractive methods. AM processes such as Selective Laser Melting (SLM), Directed Energy Deposition (DED) Selective Laser Sintering (SLS), Selective Heat Sintering (SHS) and Electron Beam Melting (EBM) have the capability to manufacture components which were previously impossible to manufacture using traditional methods[1].

The technology is still in early maturity stages and in order to reach its anticipated potential, the crucial issue to address is its robustness and this can be done with the development of advanced sensing and imaging methods that are able to cope with the extreme environments of the manufacturing process, as well as the restricted access to the various parts of the system.

Ultrasound is a powerful non-destructive testing technique that has been developed for many decades and it is now a mainstream testing method for applications ranging from aerospace to medicine. One of the most important events in ultrasonics is the development of ultrasonic phased arrays. This is the technology at the heart of sonars and medical ultrasonic equipment and it has led to profound impact in science, medicine and society, which is due to the increased imaging quality offered by phased arrays. However, transducer based ultrasonic phased arrays have certain drawbacks: it is a contact technique, requiring a coupling medium, an immersion tank may be needed. In addition, they have a considerable footprint, they are not suited for restricted access and their delicate electrical connections and packaging would not withstand extreme environments. All these are barriers when it comes to AM process monitoring.

Laser ultrasonics is a technique that uses lasers for the generation and detection of ultrasound[2, 3]. The non-destructive, thermoelastic expansion of the component, caused by the pulsed laser light absorption, generates ultrasonic waves. The detection of the waves is usually done optically, using some type of optical interferometer[4]. The advantages of laser ultrasonics over conventional ultrasonic transducers is that it is a remote and couplant free technique that can cope with the extreme environments of the manufacturing process and places of restricted access. It is also a broadband technique and all modes of ultrasonic waves (e.g. longitudinal, shear, surface waves) are excited.

Laser induced ultrasonic phased arrays could offer ultrasonic images of increased quality, just like the transducer based ones. However, in conventional phased arrays, there are rows of transducers (typically number of elements >60) that are able to transmit and detect ultrasound, focusing and steering the ultrasonic beam, detecting the echoes and forming the image. Following the same philosophy with laser ultrasonics would require several laser beams and as many optical interferometric detectors, making the setup very hardware demanding[5, 6, 7]. The alternative is to perform the imaging in post processing. The synthetic aperture focusing technique (SAFT) has been used by previous authors[8, 9], however it has only been used at the destructive, ablation regime. The authors of the present paper have recently demonstrated Laser Induced Phased Arrays (LIPAs) by means of Full Matrix Capture (FMC) and using the Total Focusing

Method as imaging algorithm, at the non-destructive, thermoelastic regime[10,11]. The present paper shows how LIPAs can be used for ultrasonic imaging of AM components, demonstrating the potential of the technique for inline process monitoring.

2. Background

2.1 Basics of Laser Ultrasonics

In laser ultrasonics, the light of a pulsed laser is focused on the surface of the component. At the non-destructive, thermoelastic regime and in metals, the laser light is absorbed. There is localised heating of the surface of the component, causing it to expand rapidly at times that are comparable to the rise time of the laser pulse which—for the cases considered here—is in the order of 1 ns. As the laser energy is absorbed in a layer much thinner than the ultrasonic wavelength (a few nanometres in aluminium), the bandwidth of the generated wave depends on the temporal characteristics of the laser pulse and is broadband. Longitudinal, shear and surface acoustic waves are generated. In the experiments described in this paper, the laser light was focused in a line. In this case, the angular dependence of the amplitude of the longitudinal and the shear waves can be found in Stratoudaki *et al.* (2016)[10]. For aluminium, the directivity pattern of the longitudinal waves has its maxima at ±64° observation angle with respect to the normal and for shear waves the maxima are at ±30° observation angle with respect to the normal[10]. In the non-destructive, thermoelastic regime, which was of interest to this study, shear waves are more efficiently produced than longitudinal waves, with approx. 10 times more energy radiated by the shear wave than the longitudinal, for the case of aluminium[12]. This is the reason for choosing shear waves for the experimental analysis in our paper.

A laser vibrometer was used for ultrasonic detection in our experiments, which was sensitive to the out-of-plane ultrasonic component. Its sensitivity to longitudinal and shear waves, as a function of angle can be found in Stratoudaki *et al.* (2016)[10]. For the case of aluminium, the sensitivity pattern for the longitudinal waves displays uniform response with respect to angle, while the sensitivity for the shear waves has maxima at ±36° observation angle with respect to the normal.

2.2 Full Matrix Capture and Total Focusing Method

The Full Matrix Capture (FMC) is a data acquisition method developed for conventional ultrasonic arrays. In this method, the waveform from every possible combination of transducer/receiver of an n element array is captured and forms an n × n matrix, the full matrix[13]. As the directivity and sensitivity patterns have angular dependence, in laser ultrasonics, a forward model was created that is able to predict the FMC data set and can simulate the response from one or more small targets, while only first order scattering is considered. In the frequency, ω, domain, the response to the j_{th} target for generated and detected mode T, for shear, can be written as[10]:

$$H_{gdj}^{TT}(\omega) = \frac{G_T(\theta_{gj}) D_T(\theta_{dj})}{(|\mathbf{d}_{gj}||\mathbf{d}_{dj}|)^{1/2}} A_j(\theta_{gj}, \theta_{dj}, \omega) \exp\left[-i\omega \left(\frac{|\mathbf{d}_{gj}| + |\mathbf{d}_{dj}|}{c_T} \right) \right] \quad (1)$$

where G_T and D_T describe the directivity and sensitivity patterns, θ_{gj} and θ_{dj} are the angles (relative to the surface normal) of the rays between the generation and detection positions and the target, $\mathbf{d}_{gj}$ and $\mathbf{d}_{dj}$ are the corresponding path lengths, and A_j (θ_{gj}, θ_{dj}, ω) is the angular dependent response or scattering matrix [Zhang2008] of the target.
The FMC data set can then be post processed with a range of imaging algorithms, including the Total Focusing Method (TFM)[13]. The TFM for laser ultrasonics should take into account the angular dependence of the generation and detection patterns and this is done by introducing apodisation terms in the imaging algorithm, as described in Stratoudaki *et al.* (2017)[11]. Apodisation introduces a weighting factor at the contribution of each captured ultrasonic signal, in the TFM imaging algorithm. As a result, the intensity, $I(\mathbf{r})$ at any point in the image is given by[11]:

$$I(\mathbf{r}) = \left| \sum_{g=1}^{n} \sum_{d=1}^{n} Z_g(r) Z_d(r) s_{gd}(t_{gd}(\mathbf{r})) \right| \tag{2}$$

where Z_g and Z_d are the apodisation coefficient for generation and detection, respectively[11], $s_{gd}(t)$ are the signals collected during the experiment, digitally filtered, and t_{gd} is the time delay term.
The response model described in equ. (1) can be combined with the adapted TFM description in equ. (2), to produce the sensitivity image[11], $E(\mathbf{r})$, which describes the amplitude expected from a perfect point target:

$$E(\mathbf{r}) = \left| \sum_{g=1}^{n} Z_g(\mathbf{r}) \frac{G_T(\theta_g(\mathbf{r}))}{\sqrt{d_g(\mathbf{r})}} \sum_{d=1}^{n} Z_d(\mathbf{r}) \frac{G_T(\theta_d(\mathbf{r}))}{\sqrt{d_d(\mathbf{r})}} \right| \tag{3}$$

The normalised TFM image ($N(\mathbf{r})$) is also introduced as the ratio between TFM image, $I(\mathbf{r})$, and the sensitivity image, $E(\mathbf{r})$[11].

$$N(\mathbf{r}) = \frac{I(\mathbf{r})}{E(\mathbf{r})} \tag{4}$$

The normalised TFM image has uniform sensitivity but non-uniform noise, as opposed to the TFM image ($I(\mathbf{r})$) which has uniform noise but non-uniform sensitivity.

3. Experimental setup and sample preparation

The experimental setup is shown in figure 1. The ultrasonic generation laser was a Nd:YVO pulsed laser, emitting at 1064 nm wavelength, with a 1 ns pulse duration and repetition rate of 5 KHz. The laser energy in front of the sample was 0.1 mJ per pulse. The laser beam was focused by means of a cylindrical lens, to a line of 5 mm height and 0.2 mm width. A Polytech vibrometer (OFV-534 head with OFV-5000 controller) was used to detect the ultrasonic signal. The light of the 633 nm HeNe laser that the detection laser emits, had a power of <1mW and was focused to a 0.04 mm diameter spot. The detection laser was aligned with the middle of the generation line source.

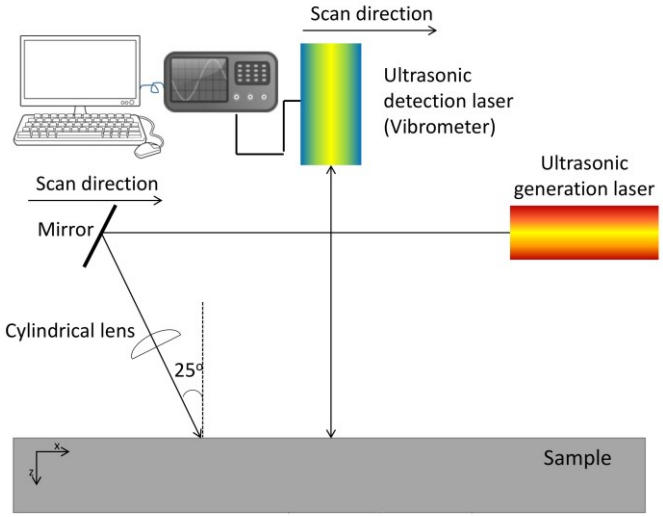

Figure 1. Experimental setup. Side view.

The sample was built using Selective Laser Melting (SLM), with Realiser SLM50. It was made by melting Aluminium powder on top of a standard Realiser 10 mm built plate, made of bulk Aluminium. The built was 40 x 20 x 10 mm, as can be seen in figure 2. The built design included six side through holes. The holes were designed to replicate side drilled holes, while having similar characteristics to defects found within SLM components, such as internal surface roughness and backfilling. The smaller defects (designed to be 0.5 mm diam.; white arrows in figure 2 (a)) were sized to replicate the same order of magnitude found in classic SLM defects[14]. The larger defects (designed to be 1 mm diam.; black arrows in figure 2 (a)) were sized to replicate small features commonly manufactured using processes such as SLM. The holes were spaced equally at increments of 5mm horizontally. The shallowest hole was placed 6 mm from the base of the build and the defects following that were placed at depth increasing by 2 mm per hole. A 129 element LIPA, with 194 μm element spacing, was synthesised at the back of the built plate, which was given a polished surface finish in order to increase the optical reflection from the detecting laser vibrometer. The back of the built plate and the position where the LIPA was synthesised can be seen in figure 2 (b). The hole closest to the back of the built plate was at a depth of 16 mm and the hole furthest from the back of the built plate was at a depth of 26 mm.

A 1 MHz High Pass analogue filter and a 20 MHz Low Pass analogue filter were used during data acquisition. Each captured waveform was averaged 500 times. During the post processing, digital filtering of the signal was performed in order to maximize the SNR(10) (Stratoudaki 2016). The digital filter applied had central frequency of 3 MHz, with 100% bandwidth, at -40 dB. In order to synthesize the LIPA, the generation and the detection laser beams were scanned in turns, while the sample remained stationary: The detection laser was scanned across all consecutive element positions, while the generation laser remained focused at one position. Then the generation laser was focused to another element position and the detection laser was scanned again across all element positions. This was repeated until the generation beam had irradiated all array element positions.

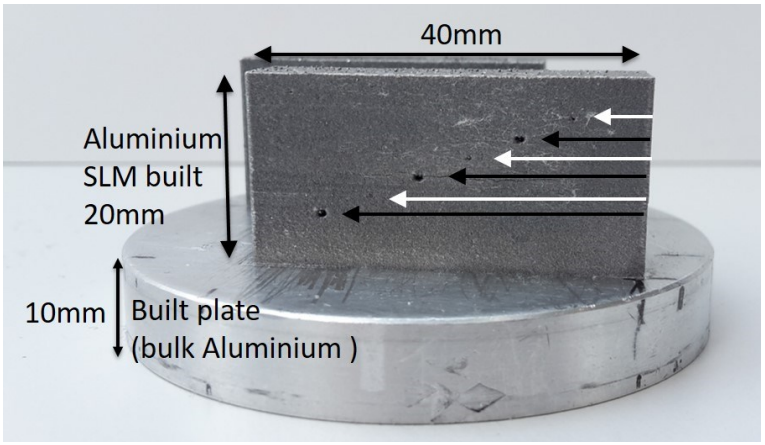

(a)

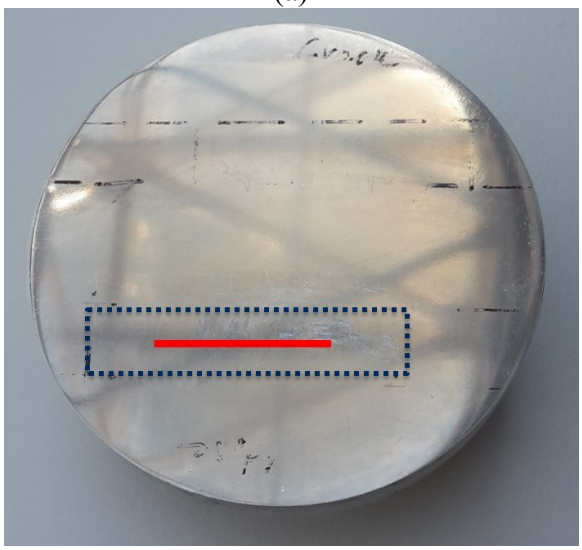

(b)

Figure 2. AM sample: (a) Aluminium built sample (top) with built plate (top and bottom) and six side through holes of 1 mm diam., (black arrows) and 0.5 mm diam., (white arrows). Side view. (b) Back side of aluminium built plate, as seen from bottom. The red line indicates the position where the LIPA was synthesised. The dotted rectangle marks the position of the AM aluminium built, located at the opposite side.

4. Experimental results

Figure 3 shows the normalized TFM image ($N(\mathbf{r})$) from the AM sample, using the FMC from signals captured from the back of the built plate. The shear-shear wave arrival was used at the TFM focusing law and a shear wave velocity of c_T=3100 m/s was used in equ. (2), equ. (3) and equ. (4).

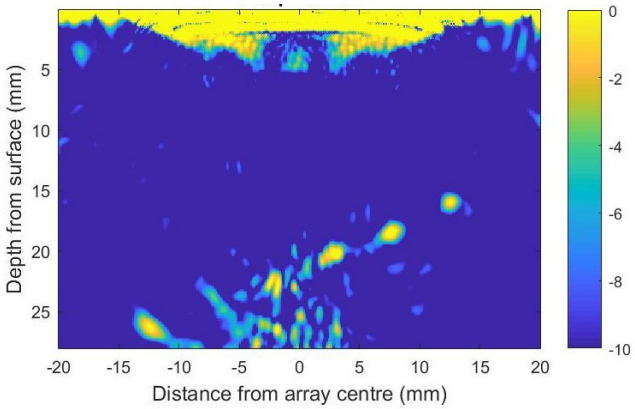

Figure 3. Normalised TFM image of AM sample with six side holes using a LIPA with 129 elements, shear-shear wave arrival. A digital filter of 3 MHz was used. The dynamic range has been included at the right (dB scale).

All six side holes can be detected in figure 3, although the 1 mm diam. hole at -7 mm from the array centre and at 24 mm depth from the back of the built plate, is just above the noise level.

A transducer based phased array was also used for FMC and TFM imaging of the AM sample. The transducer array had 128 elements which were transmitting and receiving longitudinal waves at 10 MHz frequency. The TFM image can be seen in figure 4. All six holes of the AM sample are detected. Figures 3 and 4 are not directly comparable as the transducer based phased array was using different wave mode and different frequency. In addition, the transducer based data were collected with the phased array in contact with the sample and using a coupling medium, whereas the LIPA is a remote, couplant free technique.

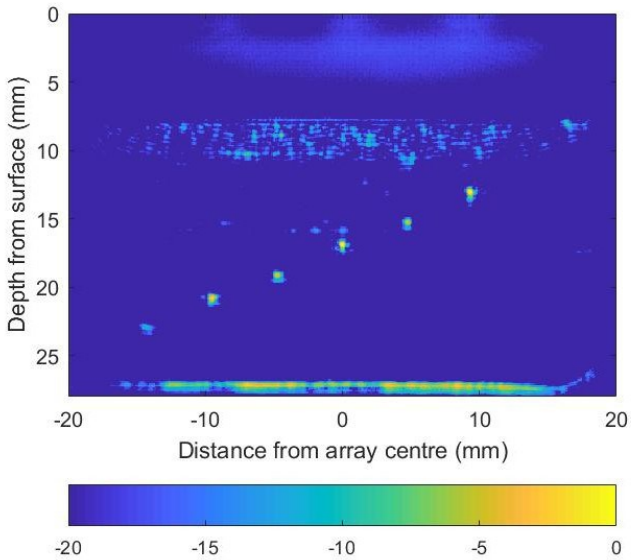

Figure 4. TFM image of AM sample with six side holes using a transducer based phased array with 128 elements and 10 MHz frequency. Longitudinal-longitudinal wave arrival. The dynamic range has been included at the bottom (dB scale)

4. Conclusions

LIPAs synthesised in post processing, have been successfully used for remote, couplant free ultrasonic imaging of an additive manufactured component, with a simple experimental setup. FMC data acquisition was done, followed by post processing using the TFM, which has been adapted to laser ultrasonics: apodisation terms were introduced which take into account the directivity and sensitivity patterns of laser ultrasonics. Defects as small as 0.5 mm in diameter and located as deep as 26 mm below the surface of the sample, have been detected. Remote ultrasonic imaging with LIPAs opens the door to non-destructive imaging for AM. Our next step is to integrate LIPAs into the AM process.

References

1. B. P. Conner, G. P. Manogharan, A. N. Martof, L. M. Rodomsky, C. M. Rodomsky, D. C. Jordan, J. W. Limperos, ‘Making sense of 3-D printing: Creating a map of additive manufacturing products and services’, Additive Manufacturing, Vol 1-4, pp 64–76, 2014.
2. S. J. Davies, C. Edwards, G. S. Taylor, and S. B. Palmer, 'Laser generated ultrasound: its properties, mechanisms and multifarious applications', J. Phys. D: Appl. Phys., Vol 26, pp 329-348, 1993.
3. C. B. Scruby and L. E. Drain, 'Laser Ultrasonics, Techniques and Applications', Bristol, UK: Adam Hilger, 1990.
4. J. P. Monchalin, 'Optical detection of ultrasound', IEEE Trans. Ultrason., Ferroelectr., Freq. Control, Vol 33, No 5, pp 485–499, 1986.
5. J.S. Steckenrider, T.W. Murray, J.B. Deaton Jr. and J.W. Wagner, ‘Sensitivity enhancement in laser ultrasonics using a versatile laser array system’, J. Acoust. Sot. Am., Vol 97, pp 273-279, 1995.
6. T. W. Murray, J. B. Deaton, Jr., and J. W.Wagner, ‘Experimental evaluation of enhanced generation of ultrasonic waves using an array of laser sources’, Ultrasonics, Vol 34, pp 69-77, 1996.
7. M.-H. Noroy, D. Royer and M. Fink, ‘The laser-generated ultrasonic phased array: Analysis and experiments’, J. Acoust. Soc. Am., Vol 94, pp 1934-1943, 1993.
8. A. Blouin, D. Levesque, C. Neron, D. Drolet and J.-P. Monchalin, ‘Improved resolution and signal-to-noise ratio in laser-ultrasonics by SAFT processing’, Opt. Express, Vol 2, pp 531-539, 1998.
9. D. Levesque, A. Blouin, C. Neron, J.-P. Monchalin, ‘Performance of laser-ultrasonic F-SAFT imaging’, Ultrasonics, Vol 40, pp 1057–1063, 2002.
10 T. Stratoudaki, M. Clark, and P. D. Wilcox. ‘Laser induced ultrasonic phased array using full matrix capture data acquisition and total focusing method’, Opt. Express, Vol. 24, no. 19, pp 21921–21938, 2016.
11 T. Stratoudaki, M. Clark, P.D. Wilcox, ‘Adapting the Full Matrix Capture and the Total Focusing Method to laser ultrasonics for remote non destructive testing’ IEEE International Ultrasonics Symposium, Washington, DC, September 06-09, 2017.
12 L. R. F. Rose, ‘Point-source representation for laser-generated ultrasound’, J. Acoust. Soc. Am., Vol. 75, pp 723–732, 1984.

13 C. Holmes, B. W. Drinkwater, P. D. Wilcox, ‘Post-processing of the full matrix of ultrasonic transmit-receive array data for non-destructive evaluation’, NDT&E Int., Vol. 38, no. 8, pp 701-711, 2005.
14 H. Taheri, M. R. B. M. Shoaib, L. W. Koester, T. A. Bigelow, P. C. Collins, L. J. Bond, ‘Powder based additive manufacturing - A review of types of defects, generation mechanisms, detection, property evaluation and metrology’, Int. J. Additive and Subtractive Materials Manufacturing, Vol. 1, no. 2, pp. 172–209, 2017.